A FULLY DYNAMIC APPROACH FOR TURBULENCE AND COMBUSTION MODELLING: SYSTEMATIC ASSESSMENT STUDY ON FIRE PLUMES WITH VARIABLE HEAT RELEASE RATE

G. Maragkos and B. Merci
Georgios.Maragkos@UGent.be
Department of Structural Engineering and Building Materials, Ghent University - UGent, St. Pietersnieuwstraat 41, B-9000 Ghent, Belgium

Abstract
A fully dynamic approach for turbulence and combustion modelling is presented in the context of fire flames. The approach is evaluated in a series of medium-scale fire plume scenarios with different burner configurations and varying heat release rates. Through the use of Large Eddy Simulations (LES), it is investigated whether the proposed approach can accurately predict the fire plume dynamics on different grid sizes by comparing the numerical predictions against experimental data involving both first and second order statistics. Furthermore, it is investigated whether the predicted turbulence model parameters are in line with the theoretically derived values as often used in the literature in the context of fire simulations.

Introduction
Fires represent a significant hazard in today's society, with potential impact on human lives and properties, given the abundance of combustible materials found in buildings. The use of Computational Fluid Dynamics (CFD) is, within this context, a very useful tool for fire safety engineers used for simulating complex scenarios that would, otherwise, be difficult to analyse with simplified models. However, the inherent coupling of turbulence, combustion and radiation modelling poses significant challenges for CFD codes, particularly given the wide range of time and length scales involved in most fire scenarios (e.g., involving large compartments or high-rise buildings). In addition, many of the models (e.g., related to turbulence and combustion) used in fire modelling have been developed for combustion applications where the flows are significantly more turbulent (i.e., for flows with much higher Reynolds number). For this reason, the theoretically derived model parameters might not necessarily be representative of the turbulence levels present in fire scenarios. The use of dynamic models, which could adjust their model parameters depending on the local flow conditions, could be a good alternative in order to improve accuracy of fire simulations. Nevertheless, dynamic models have to be able to perform accurately on a wide range of grid sizes if they are to be useful for fire modelling.

The paper focuses on Large Eddy Simulations (LES), considering various medium-scale fire plumes, and uses a fully dynamic approach (i.e., no model constants) related to turbulence and combustion modelling. Radiation is considered using the radiative fraction approach in order to decouple, to the extent possible, radiation from turbulence/combustion modelling. The accuracy of the proposed approach is evaluated on different grid sizes and the predictions are compared to available experimental data in the literature. In addition, the predicted turbulence model parameters are compared against the theoretical values reported in the literature. The present paper is a continuation of the authors' previous work on the same topic [1] and extends the proposed approach making it fully dynamic in terms of turbulence and combustion modelling.

Modelling
The CFD code FireFOAM 2.2.x, which solves the Navier-Stokes equations along with transport equations for species mass fractions and sensible enthalpy, is used. An overview of the govern-

ing equations considered is given below [1]:

$$\frac{\partial \overline{\rho}}{\partial t} + \nabla \cdot (\overline{\rho}\widetilde{u}) = 0 \tag{1}$$

$$\frac{\partial (\overline{\rho}\widetilde{u})}{\partial t} + \nabla \cdot (\overline{\rho}\widetilde{u}\widetilde{u}) = -\nabla \overline{p} + \nabla \cdot \left[\mu_{eff} \left(\nabla \widetilde{u} + (\nabla \widetilde{u})^T - \frac{2}{3}(\nabla \cdot \widetilde{u}) I \right) \right] + \overline{\rho} g \tag{2}$$

$$\frac{\partial (\overline{\rho}\widetilde{Y}_k)}{\partial t} + \nabla \cdot (\overline{\rho}\widetilde{u}\widetilde{Y}_k) = \nabla \cdot \left[\overline{\rho} \left(D_k + \frac{\nu_{sgs}}{Sc_t} \right) \nabla \widetilde{Y}_k \right] + \overline{\dot{\omega}_k'''} \tag{3}$$

$$\frac{\partial (\overline{\rho}\widetilde{h}_s)}{\partial t} + \nabla \cdot (\overline{\rho}\widetilde{u}\widetilde{h}_s) = \frac{\overline{Dp}}{Dt} + \nabla \cdot \left[\overline{\rho} \left(\alpha + \frac{\nu_{sgs}}{Pr_t} \right) \nabla \widetilde{h}_s \right] - \nabla \cdot \overline{\dot{q}_r''} + \overline{\dot{q}_c'''} \tag{4}$$

where $\overline{\rho}$ is the density, $\widetilde{u}$ is the velocity, $\overline{p}$ is the pressure, $\mu_{eff} = \mu + \mu_{sgs}$ is the effective (i.e., molecular plus sub-grid scale) dynamic viscosity, I is the identity tensor, g is the gravitational acceleration, $\widetilde{Y}_k$ is the species mass fraction, D_k is the species mass diffusivity, Sc_t is the turbulent Schmidt number, $\overline{\dot{\omega}_k'''}$ is the species reaction rate, $\widetilde{h}_s$ is the sensible energy, α is the thermal diffusivity, Pr_t is the turbulent Prandtl number, $\overline{\dot{q}_r''}$ is the radiative heat flux, $\overline{\dot{q}_c'''} = \Delta H_c \, \overline{\dot{\omega}_F'''}$ is the heat release rate per unit volume due to combustion and ΔH_c is the heat of combustion of the fuel. All molecular thermophysical properties are temperature-dependent, differential diffusion is ignored, a unity Lewis number assumption is used (i.e., $D_k = D = \alpha$) and $Sc_t = Pr_t$.

Turbulence

The dynamic Smagorinsky model [2] is used for turbulence modelling, calculating the sub-grid scale viscosity as:

$$\mu_{sgs} = \overline{\rho}(c_s \Delta)^2 |\widetilde{S}| \tag{5}$$

where Δ is the filter width (i.e., cube root of the cell volume) and $\widetilde{S}$ is the (resolved) strain rate. The model parameter, c_s, is calculated as:

$$c_s^2 = \frac{\frac{1}{2}\langle L_{ij} M_{ij} \rangle}{\langle M_{ij} M_{ij} \rangle} \tag{6}$$

with the brackets denoting averages computed as local averages of their face values. The Leonard term is defined as $L_{ij} = \widehat{\overline{\rho}\widetilde{u}_i\widetilde{u}_j} - (\widehat{\overline{\rho u_i}}\,\widehat{\overline{\rho u_j}})/\widehat{\overline{\rho}}$, $\beta_{ij} = -\widehat{\Delta}^2 \widehat{\overline{\rho}} |\breve{\widetilde{S}}| (\breve{\widetilde{S}}_{ij} - \delta_{ij} \breve{\widetilde{S}}_{kk}/3)$, $\alpha_{ij} = -\Delta^2 \overline{\rho} |\widetilde{S}| (\widetilde{S}_{ij} - \delta_{ij} \widetilde{S}_{kk}/3)$ and $M_{ij} = \beta_{ij} - \widehat{\alpha_{ij}}$. The hat denotes the application of a top-hat test filter (i.e., set to $\sqrt{6}$ times the LES filter [3]) while $\breve{f} = \widehat{\overline{\rho f}}/\widehat{\overline{\rho}}$.

The sub-grid kinetic energy is estimated as [4]:

$$k_{sgs} = c_I \Delta^2 |\widetilde{S}|^2 \tag{7}$$

with the model parameter c_I computed dynamically as:

$$c_I = \frac{\langle \frac{1}{2} L_{kk} M_{kk} \rangle}{\langle M_{kk} M_{kk} \rangle} \tag{8}$$

with the brackets denoting averages computed as local averages of their face values, $L_{kk} = \widehat{\overline{\rho}\widetilde{u}_k\widetilde{u}_k} - \widehat{\overline{\rho}\widetilde{u}_k}\,\widehat{\overline{\rho}\widetilde{u}_k}/\widehat{\overline{\rho}}$ and $M_{kk} = \widehat{\Delta}^2 \widehat{\overline{\rho}} |\breve{\widetilde{S}}|^2 - \widehat{\Delta^2 \overline{\rho} |\widetilde{S}|^2}$.

The sub-grid scale dissipation rate is estimated as [4]:

$$\epsilon_{sgs} = \frac{c_\epsilon k_{sgs}^{\frac{3}{2}}}{\Delta} \tag{9}$$

with the model parameter c_ϵ computed dynamically as [5]:

$$c_\epsilon = \frac{(\mu_+\mu_{sgs})\widehat{\Delta}\left[\widehat{\frac{\partial\widetilde{u}_j}{\partial x_i}\frac{\partial\widetilde{u}_j}{\partial x_i}} - \frac{\partial}{\partial x_i}\left(\frac{\widehat{\overline{\rho}\widetilde{u}_j}}{\widehat{\overline{\rho}}}\right)\frac{\partial}{\partial x_i}\left(\frac{\widehat{\overline{\rho}\widetilde{u}_j}}{\widehat{\overline{\rho}}}\right)\right]^{\frac{3}{2}}}{\overline{\rho}\left(\frac{\widehat{\overline{\rho}\widetilde{u}_k\widetilde{u}_k}}{2\widehat{\overline{\rho}}} - \frac{\widehat{\overline{\rho}\widetilde{u}_k}}{2\widehat{\overline{\rho}}}\frac{\widehat{\overline{\rho}\widetilde{u}_k}}{\widehat{\overline{\rho}}}\right)} \tag{10}$$

The turbulent Prandtl number is computed as [6]:

$$Pr_t = \frac{c_s^2\langle T_j T_j\rangle}{\langle K_j T_j\rangle} \tag{11}$$

with the brackets denoting averages computed as local averages of their face values, $T_j = -\widehat{\Delta}^2\widehat{\overline{\rho}}|\breve{\widetilde{S}}|\frac{\partial\breve{\widetilde{T}}}{\partial x_j} + \Delta^2\widehat{\overline{\rho}|\widetilde{S}|\frac{\partial\widetilde{T}}{\partial x_j}}$ and $K_j = \left(\frac{\widehat{\overline{\rho u_j}\,\overline{\rho T}}}{\overline{\rho}} - \frac{\widehat{\overline{\rho u_j}}\,\widehat{\overline{\rho T}}}{\widehat{\overline{\rho}}}\right)$. The Pr_t values are clipped between 0.1 - 1.0 while the restrictions $c_\epsilon \geq 0.1$ and $c_s \geq 0$ are imposed to ensure numerical stability.

Combustion

The combustion model considers a one-step, infinitely fast, irreversible chemical reaction combined with the Eddy Dissipation Model (EDM) [7] for modelling turbulence-chemistry interactions. The EDM model calculates the fuel mass reaction rate as:

$$\overline{\dot{\omega}_F'''} = -\overline{\rho}\frac{min(\widetilde{Y}_F, \widetilde{Y}_{O_2}/s)}{\tau_{mix}} \tag{12}$$

where $\widetilde{Y}_F$ and $\widetilde{Y}_{O_2}$ are the fuel and oxygen mass fractions, respectively, and s is the stoichiometric oxygen-to-fuel ratio.

Within EDM, chemistry is considered to be fast and combustion is governed by the mixing of fuel and oxidizer through a mixing time scale model. The determination of the appropriate mixing time scale is not straightforward, given the wide range of time scales typically involved in fires (e.g., associated with diffusive, advective and/or buoyant transport). To account for the weakly turbulent conditions often present in many scenarios (e.g., above the fire source or at the base of turbulent wall fires), the model has been extended to consider mixing under different flow conditions. Turbulent mixing is assumed to be governed by sub-grid scale advection while mixing under laminar conditions is described in terms of a diffusive time scale.

The mixing time scale, τ_{mix}, is calculated as:

$$\tau_{mix} = min(\tau_{lam}, \tau_{turb}) \tag{13}$$

which considers fuel-air mixing under laminar and turbulent flow conditions, respectively.

The laminar mixing time scale is estimated as:

$$\tau_{lam} = \frac{\Delta^2}{\alpha} \tag{14}$$

The turbulent mixing time scale considers two of the most important turbulent time scales in LES: the sub-grid velocity stretching time scale (i.e., Δ/u'), associated with the turbulent flame fluctuations; and the Kolmogorov time scale (i.e., $(\nu/\epsilon_{sgs})^{1/2}$), associated with the mixing in molecular level. From this, τ_{turb} is calculated as their geometric mean [8]:

$$\tau_{turb} = \sqrt{\frac{\Delta}{u'}\left(\frac{\nu}{\epsilon_{sgs}}\right)^{1/2}} \tag{15}$$

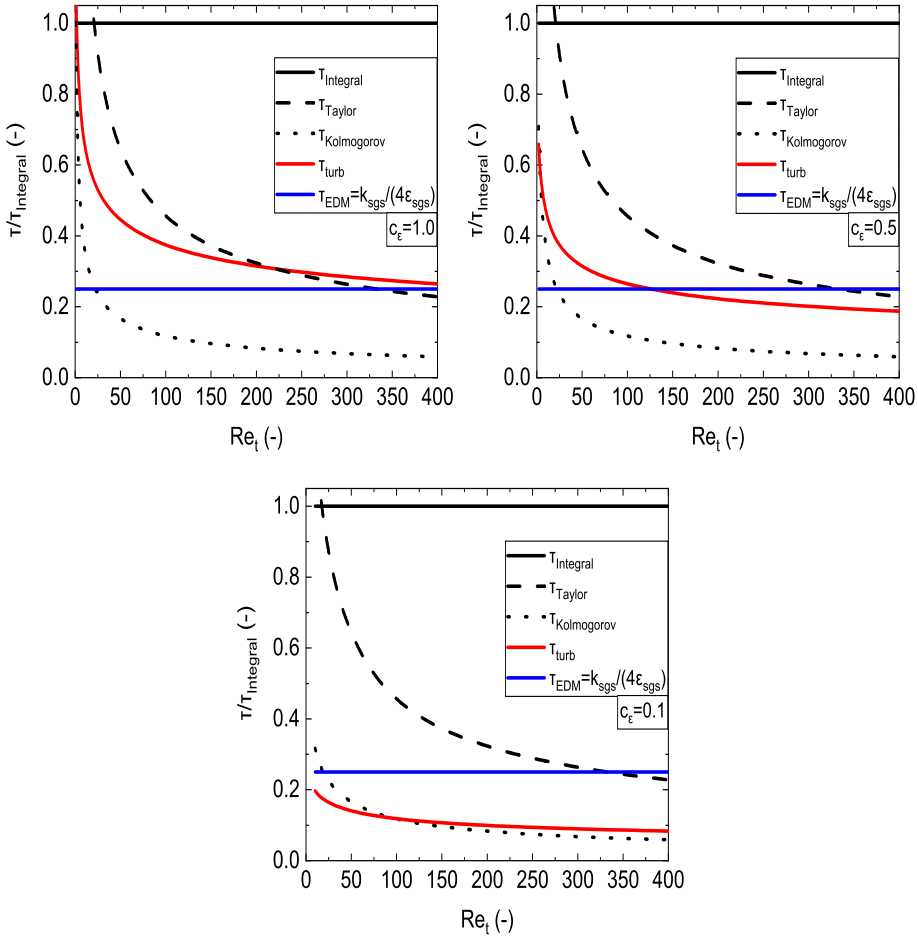

Figure 1: Comparison of the normalised time scales for different c_ϵ values as a function of the turbulent Reynolds number, Re_t.

where $u' = (2k_{sgs}/3)^{1/2}$ is the rms velocity as calculated from the sub-grid scale kinetic energy.

The variation of τ_{turb} as a function of the turbulent Reynolds number, $Re_t = k_{sgs}^2/(\nu\epsilon_{sgs})$, is presented in Figure 1 for different c_ϵ values. The Kolmogorov, Taylor and integral time scales, as well as the time scale used in the standard EDM model ($\tau_{EDM} = k_{sgs}/(4\epsilon_{sgs})$), all evaluated at sub-grid scale level, are also presented for comparison purposes. All the above-mentioned time scales have been normalized by the integral time scale. For the purpose of the analysis, a kinematic viscosity of $\nu = 17.41 \times 10^{-5}$ m^2/s, based on an average flame temperature of 1000^{o}C, has been considered. Three different values of c_ϵ have been employed (i.e., 1.0, 0.5, 0.1) in order to consider a wide range of turbulent flow conditions. When $c_\epsilon = 1$ (i.e., highly turbulent flow), τ_{turb} tends to the Kolmogorov time scale for low turbulent Reynolds values (i.e., $1 < Re_t < 25$). With increasing Reynolds number (i.e., $25 < Re_t < 200$), τ_{turb} lies approximately between the Kolmogorov and the Taylor time scales until it convergences close to the Taylor time scale for $Re_t > 200$. When $c_\epsilon = 0.5$ (i.e., reduced turbulent flow conditions), τ_{turb} exhibits a similar behaviour but the line is now shifted lower, closer to the Kolmogorov time scale line. When $c_\epsilon = 0.1$ (i.e., weakly turbulent flow), τ_{turb} follows closely the Kolmogorov time scale line indicating that molecular effects become important. The normalized ratio in the standard EDM model remains constant (i.e., 0.25) regardless of the c_ϵ value. On the other hand, the employed mixing time scale model, in combination with the fully dynamic turbulence model approach, is able to adjust the mixing time depending on the local flow conditions. Note that the grid size will have an indirect impact in the calculation of τ_{turb}, hence, the performance of the dynamic approach will be evaluated as a function of different grid sizes.

Radiation
The radiation modelling approach employed considers the radiative intensity to be a function of both spatial location and angular direction and is obtained by solving the radiative transfer equation using the finite volume discrete ordinates model. Assuming a non-absorbing and optically thin medium, the radiative heat fluxes in Equation (4) are calculated as:

$$\nabla \cdot \overline{\dot{q}_r''} = \chi_r \, \overline{\dot{q}_c'''} \tag{16}$$

where χ_r is the radiative fraction for the fuel. This simple approach guarantees that the correct amount of heat will be released per unit time due to radiation and avoids the necessity of modelling turbulence-radiation interactions (TRI), particularly if coarser grids are employed in the simulations. These aspects are useful for independent evaluation of the employed modelling approaches (related to turbulence and combustion) in the absence of uncertainties related to radiation modelling (i.e., from attempting to predict the radiative fractions).

Turbulence model constants
An overview of the different theoretically/experimentally derived turbulence model constants reported in the literature is presented in Tables 1-3. These constants involve, e.g.: c_s, used for sub-grid scale viscosity (i.e., Equation (5)); c_I, used for sub-grid-scale kinetic energy (i.e., Equation (7)); c_ϵ, used for the sub-grid scale dissipation rate (i.e., Equation (9)); and Pr_t, used in the sub-grid-scale diffusion term in the chemical species (i.e., Equation (3)) and enthalpy (i.e., Equation (4)) equations. Overall, there is a wide variation in the proposed values of the turbulence model constants. More specifically, both c_s and c_k range between 0.1-0.2, while the values of c_ϵ are in the order of 0.6-1.0. The average value of the turbulent Prandtl number, Pr_t, is the range of 0.5-0.7 for thermal plumes, while a wide range of values (i.e., 0.05-0.5) has been reported above the fire source in the case of a methanol pool fire [9]. These ranges will serve as a reference solution when comparing the turbulence model parameters obtained from the numerical simulations of the different fire scenarios presented later in the paper. When it comes to CFD modelling of fire applications, typical values for the turbulence model parameters include $c_s = 0.2$ [10], $c_k = 0.1$ [10], $Pr_t = 0.5$ [10] and $c_\epsilon = 1.0$ [1].

Table 1: Overview of c_k, c_ϵ and c_s values reported in the literature.

c_k	c_ϵ	$c_s = \left(\frac{c_k^3}{c_\epsilon}\right)^{\frac{1}{4}}$	Reference
0.042	0.634	0.104	Grötzbach (1979) [11]
0.05	1.0	0.106	Menon(1966) [12], Yoshizawa (1985) [13], Fureby (1997) [14]
0.07	1.05	0.135	Fureby (1997) [4]
0.0646	0.7	0.140	Deardorff (1974) [15], Schemm (1976) [16]
0.0666	0.7	0.143	Sommeria (1976) [17]
0.0856	0.845	0.165	Schmidt (1989) [18]
0.094	1.048	0.167	OpenFOAM
0.094	0.93	0.173	Lilly (1967) [19], Schumann (1975) [20]
0.1	0.93	0.181	Moeng (1988) [21]
0.1	0.7	0.194	Deardorff (1980) [22], Moeng (1984) [23]
0.124	0.679	0.230	Lilly (1966) [24]

Experimental test cases
Two experimental cases involving buoyancy-driven flows are considered for model validation. They are well-known in the literature since they are part of the MaCFP workshop [35]. They

Table 2: Overview of c_I values reported in the literature.

c_I	Reference
0.202	Fureby (1997) [14]
0.18	Fureby (1997) [4] Sayadi (2011) [25]
0.14	Jiménez (2001) [26]
0.0886	Yoshizawa (1986) [27] Vreman (1994) [28]

Table 3: Overview of Pr_t values reported in the literature.

Pr_t	Plume	Type	Reference
0.6	Thermal	Analytical	Craske (2017) [29]
0.62	Thermal	Experiment	Wang (2002) [30]
0.7 - 1.0	Thermal	Experiment	Shabbir (1994) [31]
0.57 - 0.71	Thermal	Experiment	Papanicolaou (1988) [32]
≈0.65	Thermal	Analytical	Launder (1975) [33]
0.2 - 0.65	Thermal	DNS	Pham (1997) [34]
0.05 - 0.5	Fire	Experiment	Weckman (1996) [9]

involve medium-scale fires with non-sooty fuels, thus eliminating any uncertainties related to soot modelling. The first case, McCaffrey's fire plumes [36], involves natural gas, issued from a 30 cm square burner, with heat release rates ranging between 14.4-57.5 kW. The second case, the UMD line burner (5 cm wide by 50 cm long) [37], involves a 50 kW methane diffusion flame in a canonical line-fire configuration. An experimental uncertainty of 10% and 20% has been assumed for the mean and rms temperatures, respectively, in this case. The combination of these test cases provides experimental data, involving both first and second order statistics, of different burner geometries and fire sizes that are useful for model validation. A more detailed documentation of the cases can be found in https://github.com/MaCFP/macfp-db.

Numerical setup

An overview of the computational domain, grid size and total number of cells considered in the simulations is outlined in Table 4. For all cases, a local grid refinement strategy (see Figure 2) is employed ensuring that a fine grid resolution is used in the near-field region of the fire plumes and up until the experimentally reported flame heights. Based on the grid requirements reported in [35] and on previous grid refinement studies on the same test cases [1], the finest grid sizes used to simulate the cases are in the order of 1 cm or less. The chosen grid sizes ensure that the ratio of the characteristic fire size, $D^* = \left(\frac{\dot{Q}}{\rho_\infty c_p T_\infty \sqrt{g}}\right)^{2/5}$, to the grid size, Δ, is in the order of 15 or higher (depending on the case), as suggested in [38]. A second order backward scheme is used for time discretization. A second order filtered linear scheme (i.e., filteredLinear2V), which limits the unboundedness of the pure central difference scheme, is used for the convective terms. For scalar transport, a TVD scheme (i.e., limitedLinear) is employed which blends central difference and upwind. For the diffusive terms, a central difference scheme is used while for the gradients a second order least squares method is applied. The choice of the numerical schemes is based on [39]. For angular discretization of the radiative transfer equation 72 solid angles are used. The cases were run for 35 sec using a varying time step limited by a maximum Courant number of 0.9, with averaging of the results over the last 30 sec.

Table 4: Overview of the setup used in the numerical simulations.

Case	McCaffrey's fire plumes [36]	UMD line burner [37]
Fuel	CH_4	CH_4
HRR ($\dot{Q}$)	14.4, 21.7, 33, 44.9, 57.5 kW	50 kW
Burner dimensions	0.3 m x 0.3 m (square)	0.5 m x 0.05 m (line)
Domain	3 m x 3.3 m x 3 m	1.6 m x 2 m x 1 m
Grid size (Δ)	1.5 cm (1 m x 2.3 m x 1 m) 3 cm (2 m x 3.3 m x 2 m) 6 cm (domain)	0.625 cm (0.6 m x 0.6 m x 0.4 m) 1.25 cm (0.8 m x 0.8 m x 0.6 m) 2.5 cm (domain)
D^*/Δ	12 - 20	not applicable
Cells	1.2 million	0.89 million
Rad. fraction (χ_r)	0.17, 0.21, 0.25, 0.27, 0.27	0.24

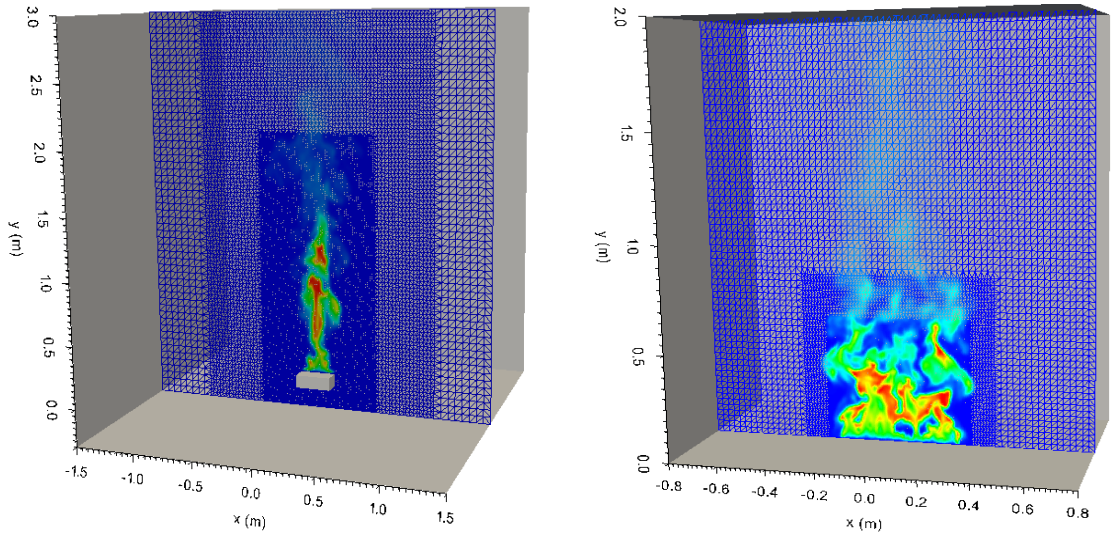

Figure 2: Domain and mesh used for the (a) McCaffrey and (b) UMD line burner case.

Results

Figure 3 presents a comparison between the numerical predictions and McCaffrey's correlations, included as dashed black lines, for the excess temperature and axial velocity. Overall, the CFD predictions with both the 1.5 cm and 3 cm grid sizes are able to reproduce, fairly accurately, the scaling laws as suggested by McCaffrey. The results on the finest grid size (i.e., 1.5 cm) do exhibit better data clustering. However the predictions between the two grid sizes remain fairly close. It is worth noting that there is scattering in the actual experimental data in the intermittent region ($0.08 < y/\dot{Q}^{2/5} < 0.2$) which is not possible to illustrate with the use of McCaffrey's correlation here. The predictions on the 6 cm grid size are not satisfactory with both the centerline excess temperatures and axial velocities being under-predicted for all heat release rates. However, this is not surprising since, in this case, there are only 5 cells across the burner, a grid resolution which is very coarse (even for an engineering type of CFD simulation).

Figure 4 presents the predicted radial mean temperature profiles at height $y = 25$ cm, along with the predicted centerline mean and rms temperatures for the UMD line burner case. Overall, the numerical simulations on the finest grid size (i.e., 6.25 mm) are able to reproduce reasonably well both the mean and rms temperatures on the centerline, as well as the width of the temperature profile at the examined height. The lack of temperature fluctuations at heights $y < 0.1$ m suggest that the fire plume is not turbulent enough just above the burner surface.

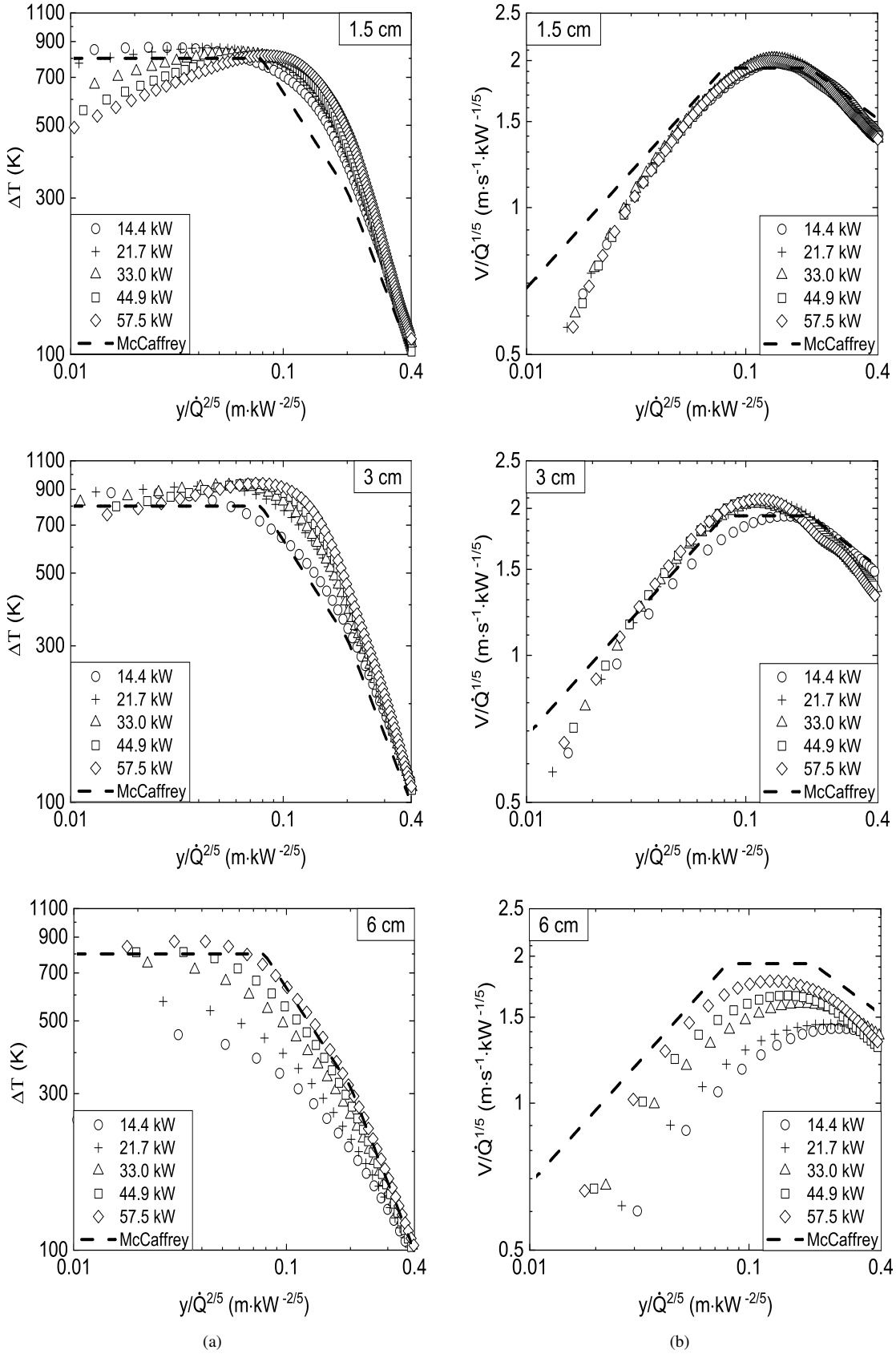

Figure 3: Centerline mean (a) temperatures and (b) axial velocities for the McCaffrey case.

The addition of turbulence at the inlet or the use of even finer grid resolution would most certainly resolve this issue. Overall, the predictions remain within the lower side of the assumed experimental uncertainty in this case. It is worth noting that the other two grid resolutions (i.e., 12.5 mm and 25 mm) used in the simulations result in only 4 and 2 cells across the width (i.e., shortest side) of the burner, respectively. These cases cannot be considered sufficient (i.e., minimum requirement), in terms of grid resolution, to simulate this scenario. Surprisingly enough, the cases also produce reasonable predictions in terms of resulting flame temperatures. The use of the fully dynamic approach is performing satisfactorily here, even with the use of coarse grid sizes.

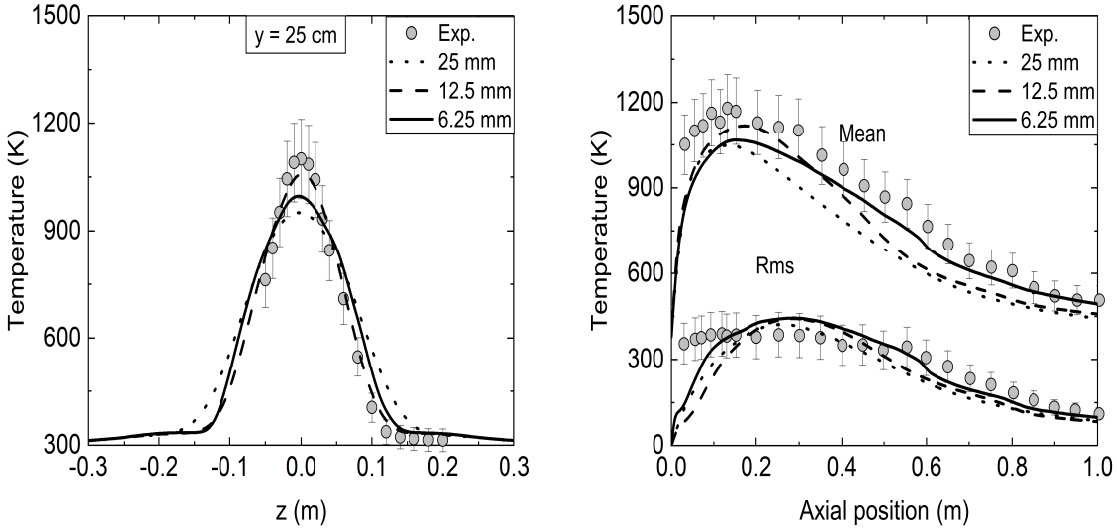

Figure 4: Predicted (a) mean radial temperatures at height $y = 25$ cm and (b) mean and rms centerline temperatures for the UMD line burner case.

Figure 5 reports the predicted turbulence model parameters for selected tests cases. Overall, low c_s values are predicted very close to the fuel source ($y < 0.1$ m) for all cases, indicating weakly turbulent conditions. The values increase with increasing downstream distance up to approximately 0.1-0.125, depending on the grid size. These values are within the typical range (i.e., 0.1-0.2) reported in the literature, but significantly lower than the theoretical values (i.e., 0.17-0.2) as widely accepted for highly turbulent flows. The increase of the c_s values with decreasing grid size indicates that the fire plumes become more turbulent. Similarly, low c_I values are predicted very close to the burner ($y < 0.1$ m) for all scenarios and subsequently remain fairly constant around 0.15-0.2, depending on the grid size. These values are in line with the values (i.e., 0.1-0.2) reported in the literature. The decrease of the c_I values with decreasing grid size indicates that more sub-grid scale kinetic energy is resolved by the simulations. A significant local variation is observed in c_ϵ, within an inlet diameter away from the fuel source (i.e., $y < 0.3$ m), with values ranging between 0.1-0.9, depending on the scenario and grid size. Subsequently, c_ϵ reaches a steady value of approximately 0.3-0.4 further downstream. Overall, the predicted values are lower than the typical range (i.e., 0.6-1.0) suggested in the literature for highly turbulent flows. Finally, Pr_t takes values in the range of 0.1-0.4 up to an inlet diameter away from the fuel source (i.e., $y < 0.3$ m) and tends to 0.5 further downstream. The relatively low Pr_t values obtained here suggest that there is enhanced transfer of enthalpy compared to transfer of momentum.

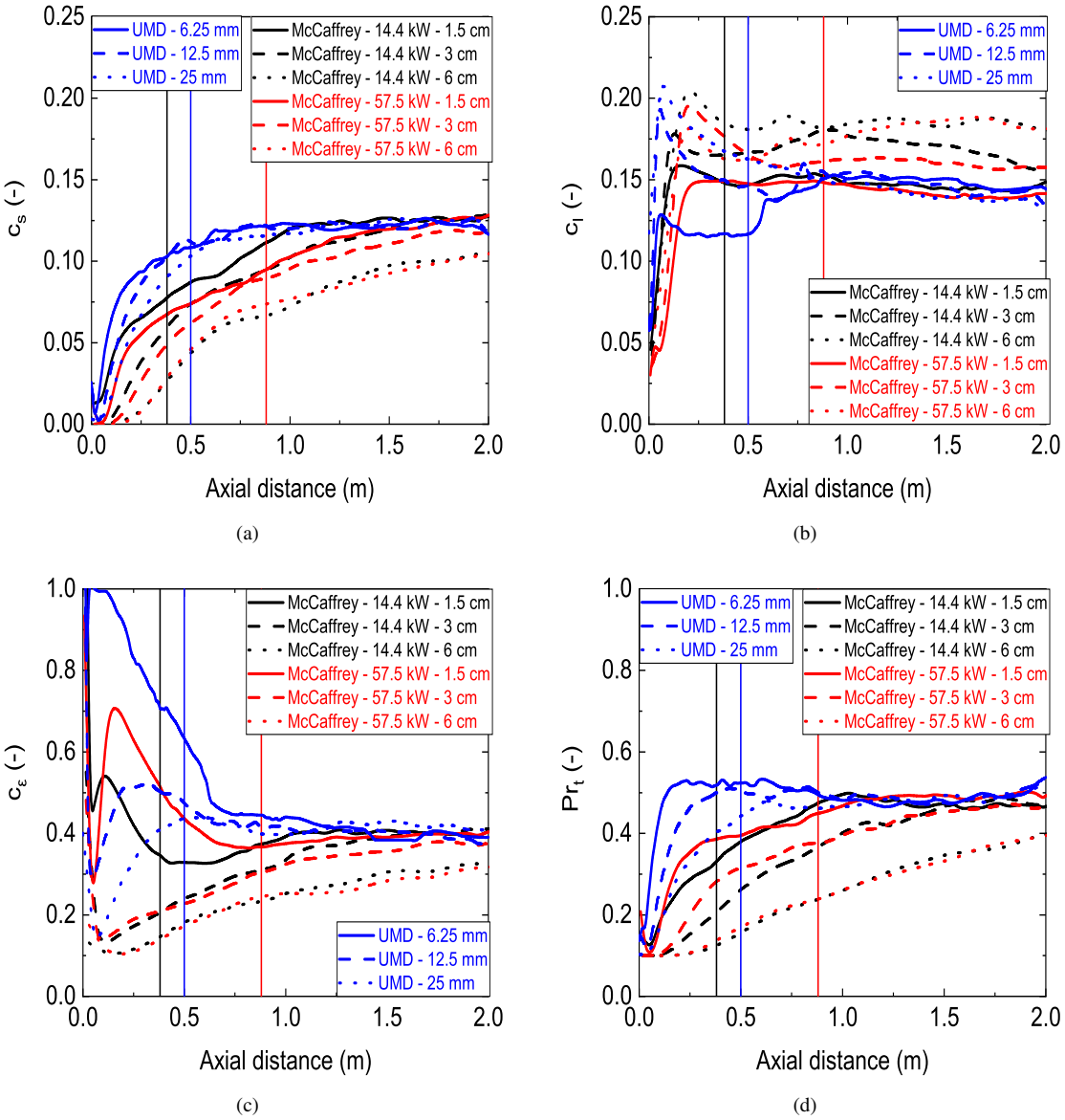

Figure 5: Predicted centerline values of (a) c_s, (b) c_I, (c) c_ϵ and (d) Pr_t as a function of grid size in the simulations. The vertical lines denote the flame height of the corresponding test case.

Conclusions

LES results, using a fully dynamic approach related to turbulence and combustion modelling, have been presented. The performance of the approach has been illustrated for different grid sizes considering two medium-scale fire plumes scenarios (i.e., McCaffrey's fire plumes and the UMD line burner). Overall, the performance of the dynamic approach was very satisfactory in the test cases applied and was able to accurately predict the fire plume dynamics (i.e., scaling of temperature and velocity) without the need of any calibration or the use of model constants. In addition, the approach predicted a significant variation in the turbulence model parameters close to the burner, where often weakly turbulent conditions exist, with the c_s (i.e., related to sub-grid scale viscosity) and c_ϵ (i.e., related to sub-grid scale dissipation rate) values being significantly lower than their theoretical values.

The present work illustrated the potential of a fully dynamic approach, with respect to turbulence and combustion modelling, towards enhancing predictive fire modelling without the need for model calibration or the use of model constants. Further evaluation of the approach, com-

bined with a predictive approach for radiation (i.e., use of WSGG type of models for predicting the radiative fraction) and the consideration of more challenging scenarios (e.g., compartment fire and/or flame spread scenarios) would be interesting to investigate in the future.

Acknowledgements
This research is funded by The Research Foundation – Flanders (FWO – Vlaanderen) through project G023221N.

References

[1] Maragkos, G., Merci, B., "On the use of dynamic turbulence modelling in fire applications", *Combust. Flame* 216: 9–23 (2020).

[2] Moin, P., Squires, K., Cabot, W., Lee, S., "A dynamic subgrid-scale model for compressible turbulence and scalar transport", *Phys. Fluids A* 3: 2746–2757 (1991).

[3] Lund, T.S., "On the use of discrete filters for large eddy simulation", in *Annual Research Briefs, Center for Turbulence Research, pp. 83–95*, NASA Ames/Stanford University (1997).

[4] Fureby, C., Tabor, G., "Mathematical and Physical Constraints on Large-Eddy Simulations", *Theoret. Comput. Fluid Dynamics* 9: 85–102 (1997).

[5] Nelson, C.C., *Simulations of spatially evolving compressible turbulence using a local dynamic subgrid model*, Ph.D. Thesis, Georgia Institute of Technology, Cambridge, UK (1997).

[6] Martin, M.P., Piomelli, U., Candler, G.V., "Sub-grid-Scale Models for Compressible Large-Eddy Simulations", *Theoret. Comput. Fluid Dynamics* 13: 361–376 (2000).

[7] Magnussen, B.F., Hjertager, B.H., "On Mathematical Modeling of Turbulent Combustion with Special Emphasis on Soot Formation and Combustion", *J. Fluid Mech.* 16: 719–729 (1977).

[8] Sabelnikov, V., Fureby, C., "LES combustion modeling for high Re flames using a multiphase analogy", *Combust. Flame* 160: 83–96 (2013).

[9] Weckman, E.J., Strong, A.B., "Experimental investigation of the turbulence structure of medium-scale methanol pool fires", *Combust. Flame* 105: 245–266 (1996).

[10] McGrattan, K., Hostikka, S., Floyd, J., McDermott, R., Vanella, M., "Fire Dynamics Simulator User's Guide", in *NIST Special Publication 1019, Sixth Edition, 2022* (2022).

[11] Grötzbach, G., Schumann, U., "Direct numerical simulation of turbulent velocity, pressure and temperature fields in channel flows", in *In Turbulent Shear Flows, vol. I, pp. 370–385 (ed. F. Durst et al.)*, Springer (1979).

[12] Menon, S., Yeung, P.K., Kim, W.W., "Effect of subgrid models on the computed interscale energy transfer in isotropic turbulence", *Comput. Fluids* 25: 165–180 (1996).

[13] Yoshizawa, A., Horiuti, K., "A Statistically-Derived Subgrid Scale Kinetic Energy Model for Large Eddy Simulation of Turbulent Flows", *J. Phys. Soc. Japan* 54: 2834–2839 (1985).

[14] Fureby, C., Tabor, G., Weller, H.G., Gosman, A.D., "A comparative study of subgrid scale models in homogeneous isotropic turbulence", *Phys. Fluids* 9: 1416–1429 (1997).

[15] Deardorff, J.W., "Three-dimensional numerical study of turbulence in an entraining mixed layer", *Bound.-Layer Meteor.* 7: 199–226 (1974).

[16] Schemm, C.E., Lipps, F.B., "Some results of a simplified three-dimensional numerical model of atmospheric turbulence", *J. Atmos. Sci.* 33: 1021–1041 (1976).

[17] Sommeria, G., "Three-Dimensional Simulation of Turbulent Processes in an Undisturbed Trade Wind Boundary Layer", *J. Atmos. Sci.* 33: 216–241 (1976).

[18] Schmidt, H., Schumann, U., "Coherent structures of the convective boundary layer derived from large-eddy simulation", *J. Fluid Mech.* 200: 511–562 (1989).

[19] Lilly, D.K., "The Representation of Small-Scale Turbulence in Numerical Simulation Experiments", in *Proceedings of IBM Scientific Computing Symposium on Environmental Sciences pp. 195-210*, Yorktown Heights, New York, USA (1967).

[20] Schumann, U., "Subgrid scale model for finite difference simulations of turbulent flows in plane channels and annuli", *J. Comput. Phys.* 18: 376–404 (1975).

[21] Moeng, C.H., Wyngaard, J.C., "Spectral analysis of large-eddy simulations of the convective boundary layer", *J. Atmos. Sci.* 45: 3573–3587 (1988).

[22] Deardorff, J.W., "Stratocumulus-capped mixed layer derived from a three-dimensional model", *Bound.-Layer Meteor.* 18: 495–527 (1980).

[23] Moeng, C.H., "A Large-Eddy-Simulation Model for the Study of Planetary Boundary-Layer Turbulence", *J. Atmos. Sci.* 41: 2052–2062 (1984).

[24] Lilly, D.K., "On the application of the eddy viscosity concept in the inertial sub-range of turbulence", in *National Center for Atmospheric Research*, Boulder, CO, USA (1966).

[25] Sayadi, T., Moin, P., "Predicting natural transition using large eddy simulation", in *Center for Turbulence Research Annual Research Briefs, 97-108* (2011).

[26] Jiménez, C., Ducros, F., Cuenot, B., Bédat, B., "Subgrid scale variance and dissipation of a scalar field in large eddy simulations", *Phys. Fluids* 13: 1748–1754 (2001).

[27] Yoshizawa, A., "Statistical theory for compressible turbulent shear flows, with the application to subgrid modeling", *Phys. Fluids* 29: 2152–2164 (1986).

[28] Vreman, B., Geurts, B., Kuerten, H., "Realizability conditions for the turbulent stress tensor in large-eddy simulation", *J. Fluid Mech.* 278: 351–362 (1994).

[29] Craske, J., Salizzoni, P., Van Reeuwijk, M., "The turbulent Prandtl number in a pure plume is 3/5", *J. Fluid Mech.* 822: 774–790 (2017).

[30] Wang, H., Law, W.K., "Second-order integral model for a round turbulent buoyant jet", *J. Fluid Mech.* 459: 397–428 (2002).

[31] Shabbir, A., George, W.K., "Experiments on a round turbulent buoyant plume", *J. Fluid Mech.* 275: 1–32 (1994).

[32] Papanicolaou, P.N., List, E.J., "Investigations of round vertical turbulent buoyant jets", *J. Fluid Mech.* 195: 341–391 (1988).

[33] Launder, B.E., "On the effects of a gravitational field on the turbulent transport of heat and momentum", *J. Fluid Mech.* 67: 569–581 (1975).

[34] Pham, M.V., Plourde, F., Doan, S., "Direct and large-eddy simulations of a pure thermal plume", *Phys. Fluids* 19: 125103 (1997).

[35] Brown, A., Bruns, M., Gollner, M., Hewson, J., Maragkos, G., Marshall, A., McDermott, R., Merci, B., Rogaume, T., Stoliarov, S., Torero, J., Trouvé, A., Wang, Y., Weckman, E., "Proceedings of the first workshop organized by the IAFSS Working Group on Measurement and Computation of Fire Phenomena (MaCFP)", *Fire Saf. J.* 101: 1–17 (2018).

[36] McCaffrey, B.J., "Purely Buoyant Diffusion Flames: Some Experimental Results", in *NBSIR 79-1910*, National Bureau of Standards, Reno, NV, USA (1979).

[37] White, J., Link, E.D., Trouvé, A.C., Sunderland, P.B., Marshall, A.W., Sheffel, J.A., Corn, M.L., Colket, M.B., Chaos, M., Yu, H.Z., "Radiative emissions measurements from a buoyant, turbulent line flame under oxidizer-dilution quenching conditions", *Fire Saf. J.* 76: 74–84 (2015).

[38] McGrattan, K., Hostikka, S., Floyd, J., McDermott, R., Vanella, M., "Fire Dynamics Simulator Technical Reference Guide Volume 3: Validation", in *NIST Special Publication 1018-3, Sixth Edition* (2022).

[39] Maragkos, G., Verma, S., Trouvé, A., Merci, B., "Evaluation of OpenFOAM's discretization schemes used for the convective terms in the context of fire simulations", *Comput. Fluids* 232: 105208 (2022).